Investigation of free vibrations of voided concrete sleepers in railway track system

S Kaewunruen* and **A M Remennikov**
School of Civil, Mining, and Environmental Engineering, Faculty of Engineering, The University of Wollongong, Wollongong, NSW, Australia

The manuscript was received on 31 January 2007 and was accepted after revision for publication on 27 July 2007.

DOI: 10.1243/09544097JRRT141

Abstract: Concrete railway sleepers in ballasted track are laid on ballast and subgrade supporting systems. Full contact between sleepers and ballast is typically assumed for analysis and design purposes. Often, voids and pockets in the sleeper/ballast contact interface form between sleepers and the ballast underneath that could cause problems to both the sleepers and the track system as a whole. The current paper investigates the effects of ballast voids and pockets on free vibration response characteristics of *in situ* railway concrete sleepers. Finite-element modelling was employed to develop a dynamic model of the railway track incorporating concrete sleepers. This model includes the dynamic interaction of sleepers and ballast as part of the free vibration analyses of the *in situ* railway concrete sleepers. Several patterns of voids and pockets underneath railway sleepers were studied. The emphasis was placed on partial and full interaction between sleepers and ballast. The information on the vertical vibration modes provides an important insight into the dynamic response of concrete railway sleepers in different void-and-pocket configurations.

Keywords: voids and pockets, *in situ* railway concrete sleepers, free vibrations, sleeper-ballast, structure-soil interaction, Timoshenko-beam on elastic foundation, shear beam, finite elements

1 INTRODUCTION

The increased congestion of highways and the current energy resources boom in Australia have increased the demand for heavier and faster trains, often at the expense of increased maintenance cost. Under heavy cycle train loads, the ballast deteriorates progressively, sometimes leading to formation of voids and pockets between sleepers and ballast. Effect of imperfect contact between railway sleepers (railroad ties) and ballast formation has not been investigated in detail so far, even though the interaction between sleeper and ballast plays an important role in railway track system dynamics. In a poor-condition track, large voids and pockets can easily be observed between sleepers and the underneath ballast, usually caused by the wet beds (highly-moist ground) from natural water springs or poor drainage (Fig. 1 [**1**]), while undetectable voids could also happen in the good-condition tracks. Since a sleeper cracks typically as a result of vibration at its resonant frequencies, it is important to investigate the effect of various sleeper/ballast contact patterns on the natural vibrations of the *in situ* railway concrete sleeper. Several studies have shown that the resonant vibrations of sleepers could affect not only the sleepers themselves, but also the wheel–rail interaction forces [**2–4**]. Dahlberg and Nielsen [**5**] used an analytical model capable of analysing the dynamic behaviour of concrete sleepers in both free–free and *in situ* conditions. Grassie [**6**] developed a two-dimensional dynamic model to perform vibration analysis of concrete sleepers in free–free conditions that was calibrated using experimental data. Both references [**5**] and [**6**] stated that the Timoshenko beam element was the best approximation for the concrete sleepers, even though the elastic properties of prestressed concrete sleepers may not be exact [**7, 8**].

**Corresponding author: School of Civil, Mining, and Environmental Engineering, Faculty of Engineering, University of Wollongong, Northfield Avenue, Wollongong, 2522 NSW, Australia. email: sakdirat@uow.edu.au or sakdirat@hotmail.com*

Fig. 1 An example of problems due to voided support

Studies of fully and partially supported sleepers have been previously performed for some sleeper/ballast configuration. Grassie and Cox [**1**] considered partially-supported sleepers as fully '*hung*' sleepers attached to the rail. The dynamic response of the deteriorated railway track was studied by Grassie and Cox [**1**] through a mathematical model. It was found that the hung sleeper could experience larger dynamic strains than the well-supported sleeper does at the critical resonant frequency at about 740 Hz. The dynamic wheel–rail contact force on an unsupported part of track was found to be higher than that on a well-supported section by up to 80 per cent. It should also be noted that packing of the ballast is also crucial to its damping performance. Plenge and Lammering [**9**] investigated the influence of a voided sleeper on the frequency response functions for a single sleeper configuration, two adjacent sleepers, and a track segment. The test programme dealt only with sleepers B70W60, designed in accordance with the German Standard. Two types of voided sleepers, dealing with single and double ends of sleepers without ballast contact, were studied in the experiments. It was found that the partially supported sleepers dramatically increase the receptance (at sleeper end) at frequencies varying from 0 to 150 Hz, while at frequencies above 150 Hz the receptance decreases slightly. Kumaran *et al.* [**10**] studied the dynamic responses of railtrack sleepers due to the wheel–rail interaction. An example called '*loss-of-contact sleeper*' was presented. In that example, there was a large space of void at the centre of the sleeper. It was found that the loss of contact gives rise to the dynamic moment magnification at the railseat, and also reduces the moment magnification at the centre. Based on the extensive literature search, very little knowledge is available on the void-and-pocket problems in relation to the railway sleepers, although these problems are the cases of the great practical concerns to the railway industry.

On this ground, there is clearly a need to carry out a study of voids and pockets in the ballast and their influences on the free vibration behaviour of the *in situ* railway concrete sleepers. By means of numerical studies, it is possible to better understand the dynamic behaviour of the railway concrete sleepers associated with the contact patterns. This paper presents the results of free vibration analyses of an *in situ* railway concrete sleeper in a track system incorporating the sleeper/ballast contact mechanisms. The dynamic effects of voids and pockets in the supporting ballast on free vibrations of the *in situ* monoblock sleepers will be investigated. The *in situ* railway concrete sleeper is modelled as a beam on elastic foundation, in this case, Winkler foundation. Finite-element approach is used in the current study utilizing a general-purpose finite-element analysis package STRAND7 [**11**]. Shear beam element feature is used in the sleeper model to take into account the shear deformation and rotational inertia. Elastic support and spring elements are utilized to represent the ballast-support system and the rail pad. Normalized characteristics of natural frequencies of the sleepers are first presented to give better insight into the dynamic stability and behaviour of *in situ* concrete sleepers associated with the diversity of voids and pockets underneath the sleepers. This information would significantly help the track engineers monitoring the structural health of track infrastructure, e.g. concrete sleepers and ballast compaction. Better understanding of the vibration characteristics of concrete sleepers would also help to understand their responses to any other transient loading. Experimental and numerical studies on the impact resistance of concrete sleepers are being conducted at the University of Wollongong, within the framework of the Cooperative Research Centre for Railway Engineering and Technologies (Rail-CRC) so as to develop the new limit states design concepts for railway prestressed concrete sleepers.

2 ANALYTICAL FORMULATIONS OF *IN SITU* RAILWAY CONCRETE SLEEPERS

Analysis and design of beams on elastic foundation is described in several books [**12**, **13**]. In case of partially supported beams under dynamic loading, one would usually employ the finite-element formulation. At present, Timoshenko beam elements are typically employed in the dynamic modelling of the sleepers, in order to obtain better agreement at higher frequencies with experimental data, since the rotatory inertia and shear deformation are included in the element formulation [**14**]. Considering an *in situ* sleeper model in Fig. 2, the equations of motion for free vibrations of the *in situ* sleeper can be written as follows [**15**]

$$\frac{\partial}{\partial x}\kappa \mathrm{AG}\left[\psi(x,t)-\frac{\partial z(x,t)}{\partial x}\right]+m_{\mathrm{s}}\frac{\partial^2 z(x,t)}{\partial x^2} + c_{\mathrm{b}}\frac{\partial z(x,t)}{\partial t}+k_{\mathrm{b}}z(x,t)=\vec{F}(x,t) \qquad (1)$$

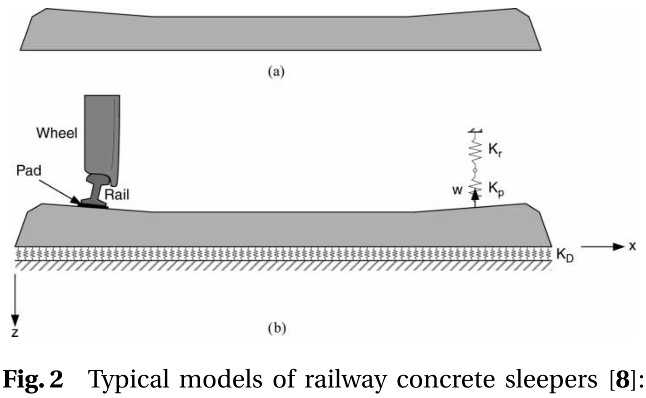

Fig. 2 Typical models of railway concrete sleepers [**8**]: (a) free–free sleeper model and (b) *in situ* sleeper model in a track system

$$\frac{\partial}{\partial x}\mathrm{EI}\left[\frac{\partial \psi(x,t)}{\partial x}\right]-\kappa \mathrm{AG}\left[\psi(x,t)-\frac{\partial z(x,t)}{\partial x}\right] - m_{\mathrm{s}}r_{\mathrm{s}}^2\frac{\partial^2 \psi(x,t)}{\partial x^2}=0 \qquad (2)$$

where

$$\vec{F}(x,t)=\sum_{i=1}^{2}\{k_{\mathrm{p}i}[w(x_i,t)-z(x_i,t)] + c_{\mathrm{p}i}[\dot{w}(x_i,t)-\dot{z}(x_i,t)]\}\delta x_i \qquad (3)$$

In equations (1) to (3), k_{b} and c_{b} represent the stiffness and damping constant of ballast support system; k_{p} and c_{p} are the stiffness and damping constant of rail pads; $z(x,t)$ is the vertical deflection of sleeper; $\psi(x,t)$ is the rotation angle of sleeper about neutral axis; EI is the effective sleeper flexural rigidity; κGA is the effective sleeper shear distortion rigidity; m_{s} is the sleeper mass per unit length; and, r_{s} is the radius of gyration of sleeper cross-section.

For the sleepers with non-uniform cross-section, the effective moment of inertia can be adopted [**6**]. This methodology is widely used due to its simplicity and convenience

$$\mathrm{EI}=\sqrt{(\mathrm{EI_r})(\mathrm{EI_c})},\quad \kappa\mathrm{GA}=\sqrt{(\kappa\mathrm{GA_r})(\kappa\mathrm{GA_c})} \qquad (4)$$

where $\mathrm{EI_c}$ and $\mathrm{EI_r}$ are sleeper flexural rigidity at centre, and at rail seats, respectively; $\kappa\mathrm{GA_c}$ and $\kappa\mathrm{GA_r}$ are the sleeper shear distortion rigidity at centre and at rail seats, respectively. The analytical solution of equations (1) to (3) has been provided for a fully supported case [**5**] and for a free–free support condition [**6**]. These solutions were used for the model validation in this work. In the finite-element (FE) model presented later, the effective stiffness (k_{e}), determined from the spring series representing steel rail and rubber rail pad stiffness (k_{r} and k_{p}, respectively), was given by $k_{\mathrm{e}}=k_{\mathrm{r}}k_{\mathrm{p}}/(k_{\mathrm{r}}+k_{\mathrm{p}})$ [**8**].

3 FINITE-ELEMENT MODEL OF SLEEPER

The dynamic finite-element model of an *in situ* railway concrete sleeper in the track system was developed to study its dynamic responses. The sleeper was modelled using 50 Timoshenko beam elements with a trapezoidal cross-section while the rail pads and the ballast system were modelled using a spring-damper element and the elastic beam support feature in STRAND7 [**11**, **16**]. The material and geometric properties of these components were adopted based on the previous investigations [**5**, **6**], as shown in Table 1. These properties were chosen because they

Table 1 Engineering properties used in the dynamic modelling

Parameter lists		
Flexural rigidity	$EI_c = 4.60$, $EI_r = 6.41$	MN/m^2
Shear rigidity	$\kappa GA_c = 502$, $\kappa GA_r = 628$	MN
Ballast stiffness	$k_b = 13$	MN/m^2
Effective stiffness	$k_e = 17$	MN/m
Sleeper density	$\rho_s = 2750$	kg/m^3
Sleeper length	2.5	m
Rail gauge	1.5	m

were identical to a particular type of concrete sleepers manufactured in Australia [**17**]. A series of natural frequency analyses was performed in order to evaluate the quality of the FE model. It was found that 50 beam elements, representing a concrete monoblock sleeper, can provide reasonable approximation of sleeper's vibration in free–free condition compared with the existing experimental data [**8**]. Spring elements were used to simulate the resilient rail pads and the ballast support system.

To validate the model, the natural frequencies of a concrete sleeper in both free–free and *in situ* conditions were calibrated against the existing analytical solutions [**5–8**]. Table 2 presents the comparison between the experimental, analytical, and finite-element analysis results. The results are found to be in a very good agreement with the previous investigations [**8**, **17–20**]. The maximum difference between the experimental and numerical results is less than 7 per cent, and less than 10 per cent between the analytical and numerical solutions. A good correlation between the analytical and finite-element analysis results is found for the shifts in natural frequencies for both free–free and *in situ* conditions. Figures 3 and 4 demonstrate the mode shapes of the concrete sleeper in free–free and *in situ* conditions. It is found that there exist the rigid body dynamic mode shapes including rotation and translation in the *in situ* condition. These modes are at the low frequency band.

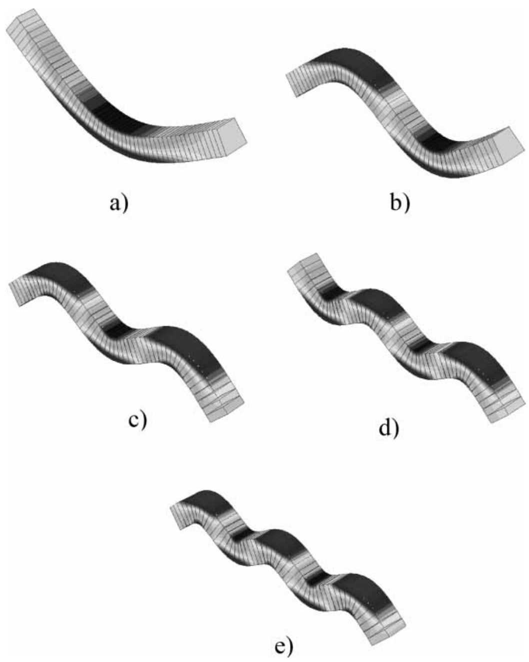

Fig. 3 Mode shapes of a free–free sleeper: (a) first mode, (b) second mode, (c) third mode, (d) fourth mode, and (e) fifth mode

4 SLEEPER/BALLAST CONTACT PATTERNS

The sleeper/ballast contact patterns considered in the eigenvalue analyses are illustrated in Fig. 5. These five situations of non-linear contact boundary conditions are of practical concern in the actual railway track problems. One way to detect these imperfections is through the vibrational testing of the track structure. Figure 5(a) shows the type of the contact problem, which is referred to as the 'central void'. In this situation, a void forms at the centre of the sleeper and extends symmetrically in both directions. The void is assumed to expand up until the sleeper becomes fully hung. This case is easily detectable by visual inspection of a poor-quality railway track. A non-dimensional parameter considered in this case,

Table 2 Comparisons of natural frequencies of ideal concrete sleeper (Hz)

	Free–free condition				*In situ* condition			
					[**5**]		This study	
Mode no.	(Experimental) [**5**]	(Analytical) [**5**]	(Analytical) [**6**]	(FEM) this study	(Analytical)	% increase	(FEM)	% increase
T	–	–	–	–	82	–	69	–
R	–	–	–	–	79	–	71	–
1	113	118	126	112	131	11	122	9.0
2	335	327	338	308	335	2.4	314	2.0
3	639	624	637	602	631	1.0	607	1.0
4	995	986	1004	994	989	0.3	997	0.3
5	1390	1391	1423	1484	1393	0.1	1486	0.1

T = translation; R = rotation

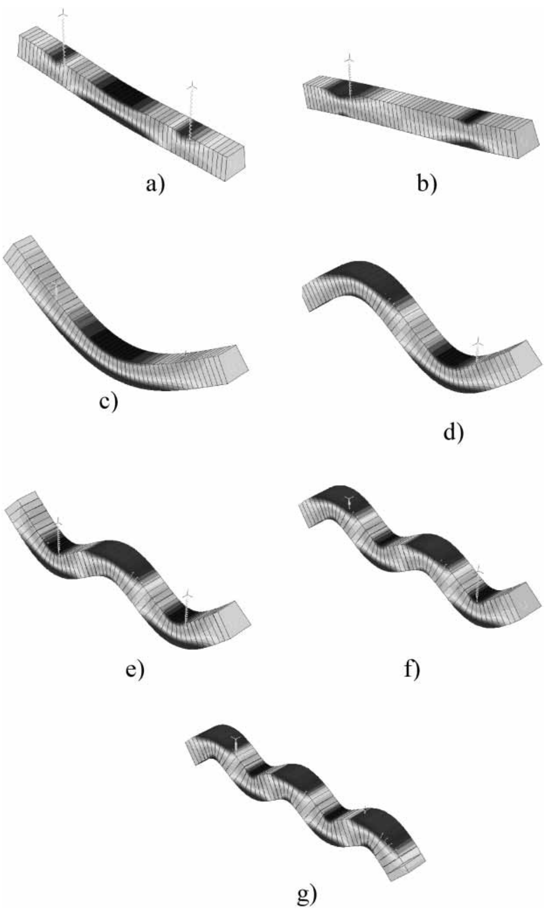

Fig. 4 Mode shapes of an ideal *in situ* sleeper: (a) translation, (b) rotation, (c) first mode, (d) second mode, (e) third mode, (f) fourth mode, and (g) fifth mode

which is the ratio of the central void length to the sleeper length, is

$$\alpha_c = \frac{L_c}{L} \tag{5}$$

Figure 5(b) presents another type of the contact pattern, which is referred to as the 'single hanging'. In this type, the hanging condition forms at one end of the sleeper. The hanging space grows incrementally from perfectly full contact to totally hung condition. This void can extend from either end of the sleeper. A non-dimensional variable for this case is the ratio of the single-side void length to the sleeper length, as follows

$$\alpha_s = \frac{L_s}{L} \tag{6}$$

The double-side hanging can also occur when the gap between the sleepers and the ballast forms at both ends. The sleeper/ballast contact in this case remains only in the middle segment of the sleeper. This contact situation is referred to as the 'double hanging' and illustrated in Fig. 5(c). The non-dimensional

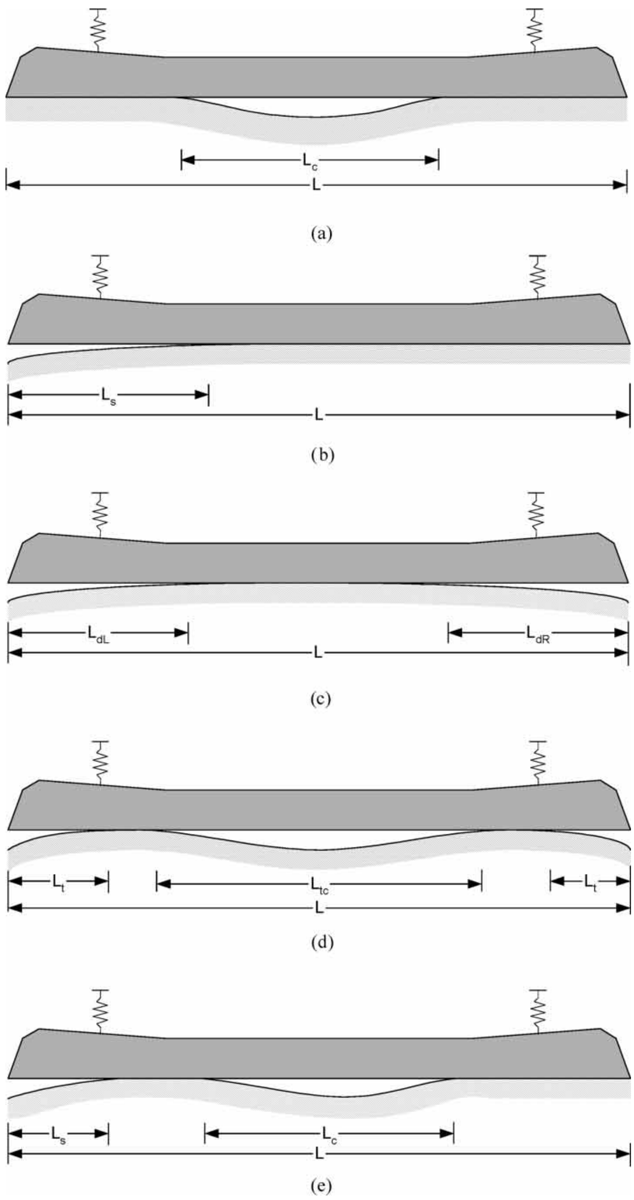

Fig. 5 Sleeper/ballast contact patterns: (a) central void, (b) single hanging, (c) double hanging, (d) triple hanging, and (e) side-central voids

parameters in this case are

$$\alpha_d = \frac{L_{dL}}{L}, \quad \beta_d = \frac{L_{dR}}{L} \tag{7}$$

The 'triple hanging' contact type is displayed in Fig. 5(d). In this contact pattern, not only do the voids form at both ends, but also there is a pocket growing up at the centre of the sleeper. Only symmetrical cases are considered in this study. The non-dimensional factors related to this contact type are

$$\alpha_t = \frac{L_t}{L}, \quad \beta_t = \frac{L_{tc}}{L} \tag{8}$$

The last contact pattern considered in the current paper is defined as the 'side-centre voids' type, and is shown in Fig. 5(e). The asymmetric contact configurations are considered in this case for which the edge hanging and the central void are supposed to form at the same time. The non-dimensional variables related to this void configuration are as follows

$$\alpha_{s-c} = \frac{L_s}{L}, \quad \beta_{s-c} = \frac{L_c}{L} \tag{9}$$

All these types of voided sleepers will be evaluated in this paper for their effects on the dynamic responses of the *in situ* railway concrete sleepers. To demonstrate the sleeper's dynamic behaviour, the normalized frequency ω_N is introduced as a ratio between the deteriorated sleeper's frequency ω_{voided} and the frequency of the *in situ* sleepers ω_{ideal} in the ideal contact condition

$$\omega_N = \frac{\omega_{\text{voided}}}{\omega_{\text{ideal}}} \tag{10}$$

5 RESULTS AND DISCUSSION

Free vibration analyses of the *in situ* railway concrete sleepers in the track system were carried out for a variety of contact patterns discussed earlier. The sleeper parameters considered for the parametric studies are given in Table 1. The results of the parametric studies for each sleeper/ballast contact pattern will be presented in separate sections below. It is noteworthy that the cracking damage of *in situ* sleepers is clearly attributed to the natural frequencies of the sleepers under dynamic loading conditions [**21**, **22**]. In order to determine the natural frequencies of the *in situ* sleepers, one would attach an accelerometer to the top surface of railway sleeper under operational excitation.

5.1 Central void

The effect of the symmetrical central void on the normalized frequencies of the *in situ* railway concrete sleeper is shown in Fig. 6. The results show that the void or pocket reduces the frequencies of all modes of vibration compared to the ideal contact condition. It is found that the support boundary conditions strongly influence the first two modes of flexural vibration, in addition to the translational and rotational modes of rigid body dynamics. Clearly, the degree of dynamic softening of the *in situ* sleeper increases as the void becomes larger, in particular for the rotational and the first bending modes of vibration. For the translational and rotational modes, the frequency reductions tend to be between 25 per cent and 30 per cent. In contrast, the bending modes are unlikely to change, except for the first bending mode that behaves softer by nearly 10 per cent in relation to the full contact situation and the second mode that declines roughly 1–2 per cent. However, it is obvious that when the small void ratios are varied from nil to about 30 per cent, the rotational frequencies are insensitive. This is because the rotational inertia cannot effectively affect the sleeper behaviour with insignificant voids. The explanation can also be extended to the first two bending modes for which the dynamic softening is not significantly affected at the small ranges of voided spaces. For the translational mode, the vertical support stiffness is reduced as the void become larger, resulting in the linear relationships between the void size and the normalized frequency. It can be seen from Fig. 6 that the void has little effect on the higher bending modes of vibration with only about 0.05–0.30 per cent difference.

5.2 Single hanging

An asymmetrical imperfection of the sleeper/ballast contact plays an interesting role in the vibration characteristics of the *in situ* railway concrete sleepers. Figure 7 presents the effect of the one end hanging condition on the normalized frequencies of the *in situ* sleeper. The translational and rotational modes seem to be affected the most by this contact condition. The dynamic hardening behaviour (frequency increment) dominates for the translational mode while the significant softening dominates the rotational mode as the void is increased by approximately 42 per cent. At about this point, the cross over (swapping) behaviour can be noticed. The normalized frequency of the translational mode drops significantly and one of the rotational modes surges up. It is found that when considering actual frequencies, these two modes cross over each other position and still sustain each other

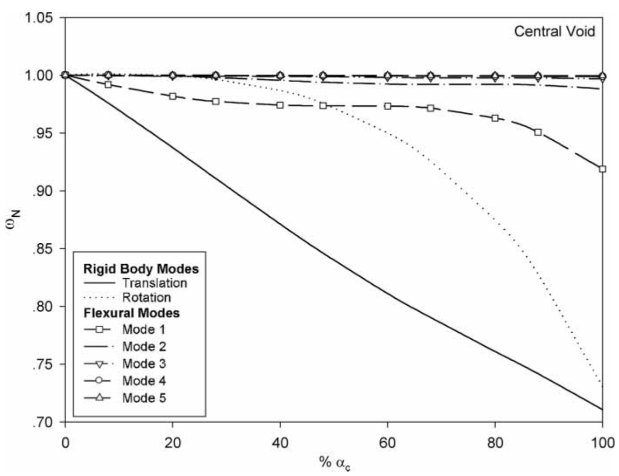

Fig. 6 Effect of central voids on natural frequencies of an *in situ* railway concrete sleeper (rigid body modes: translation and rotation)

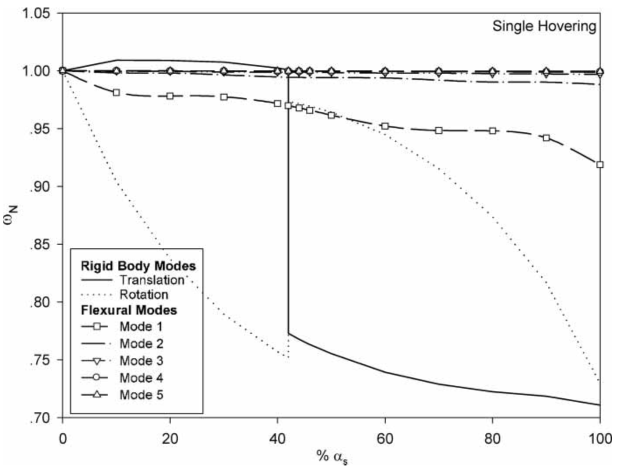

Fig. 7 Effect of single hanging on natural frequencies of an *in situ* railway concrete sleeper

non-linear trend. This behaviour is caused by the static instability occurred to the sleeper when lacking of elastic support, which results in the weight of the sleeper being transferred to the rail pad connected to the rail. At this specific void ratio, the over-hanging mass on a side of the sleeper becomes significant. Then, the new unstable static configuration forms and simultaneously affects the rigid body motions [**20**]. This instability shows the dynamic weakness in the translational mode subjected to the reduction of elastic support. Inclination of the mode shapes in translation is obvious after this point. In contrast, the sleeper rotation is constrained by the rail, which results in the higher frequency. So far, this behaviour has not been addressed in the literature on the track dynamics available to the authors. Although these two vibration modes are not critical to the track damage, it would be instructional to realize the actual behaviour of the sleepers associated with the global track behaviour when considering the effects of the deteriorated sleeper support. However, the hanging sleeper tends to have lesser effect on the flexural modes. It is also found that there are two ranges of insignificant changes in the first bending frequencies, during the void variations from 10 per cent to 30 per cent and from 60 per cent to 80 per cent in which small changes are found. It should be noted that the total softening decrements are about 9 per cent, 2 per cent, and 0.05–0.50 per cent for the first, second, and other higher bending modes, respectively.

5.3 Double hanging

In this case, both symmetrical and asymmetrical boundary conditions are considered. Figure 8 illustrates the changes in frequencies of an *in situ* railway concrete sleeper for varying percentages of voids. The symmetrical-case results are shown in Fig. 8(a). The degree of dynamic softening for the rotational modes, at the small to moderate size of voids, is the highest compared with the other modes. In particular, the small to moderate size of voids produces only about one-half of the total effects on the dynamic behaviour of each bending mode.

Figures 8(b) to (e) show the normalized effects of asymmetrical boundary conditions on the dynamic parameters of the *in situ* sleeper. At one end, the size of hanging varies in each case, while at another end it is kept constant (Fig. 8(b) for $\beta_d = 10$ per cent fixed, Fig. 8(c) for $\beta_d = 20$ per cent fixed, Fig. 8(d) for $\beta_d = 30$ per cent, Fig. 8(e) for $\beta_d = 40$ per cent, and Fig. 8(f) for $\beta_d = 50$ per cent). It is found that when α_d varies between 50 per cent and 60 per cent, the response is characterized by the swapping behaviour between the translational and rotational modes. This can be attributed to the asymmetrical contact configuration that causes dynamic instability to the system at the low range frequency responses. The new unstable static configuration would form due to the large over hanging mass. This new position distorts the mode shapes of rigid body motions, resulting in the abrupt change of normalized frequency, and vice visa. As can be seen, the above dynamic phenomena are not only affected by the values of void sizes α_d, but also by the values of β_d. However, the magnitudes of the impact rely on these parameters. Clearly, the resulting magnitudes decrease with the increased values of β_d, since the system becomes more stable and the mode shapes form more symmetrical patterns. It would be of interest to note from Fig. 8(f) that the behaviour is characterized by the mode swapping for small values of α_d. This latest case describes a transitional period between the two identical situations of single hanging at both ends. First, a void forms at the end and the system is transformed to the unstable equilibrium (similarly to the single hanging behaviour). Then, a void forms at the other end and the over hanging mass of the other side balances and stabilizes the system. The overhanging balance retrieves the more stabilized static position, resulting in the dynamic transitional period. However, it should be noted that the bending modes tend to decrease about 5–8 per cent, 1–2 per cent, and about 0.05–0.90 per cent for the first, second, and for higher modes, respectively.

5.4 Triple hanging

The dynamic behaviour of the voided concrete sleeper under triple void contact mechanism is demonstrated in Fig. 9. Only symmetrical contact configurations are presented so that there is no dynamic swapping effect in these results. As can be seen in all cases, the degrees of dynamic softening of rotational mode are higher than those of translational mode, and the normalized frequencies tend to decrease with per cent variations

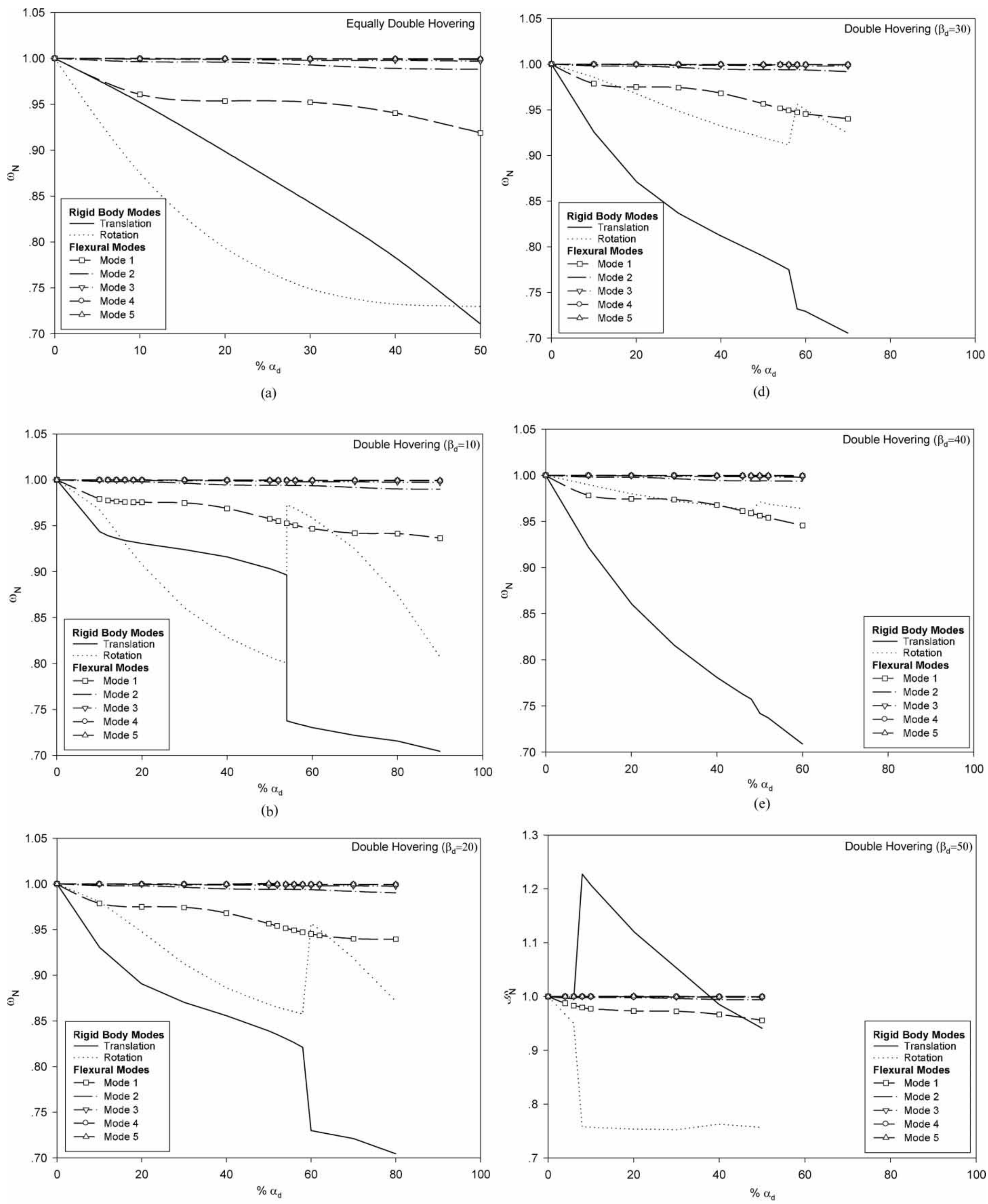

Fig. 8 Effect of double hanging on natural frequencies of an *in situ* railway concrete sleeper: (a) equal hanging at both ends ($\alpha_d = \beta_d$), (b) 10 per cent hanging at one end ($\beta_d = 10$ per cent), (c) 20 per cent hanging at one end ($\beta_d = 20$ per cent), (d) 30 per cent hanging at one end ($\beta_d = 30$ per cent), (e) 40 per cent hanging at one end ($\beta_d = 40$ per cent), and (f) 50 per cent hanging at one end ($\beta_d = 50$ per cent)

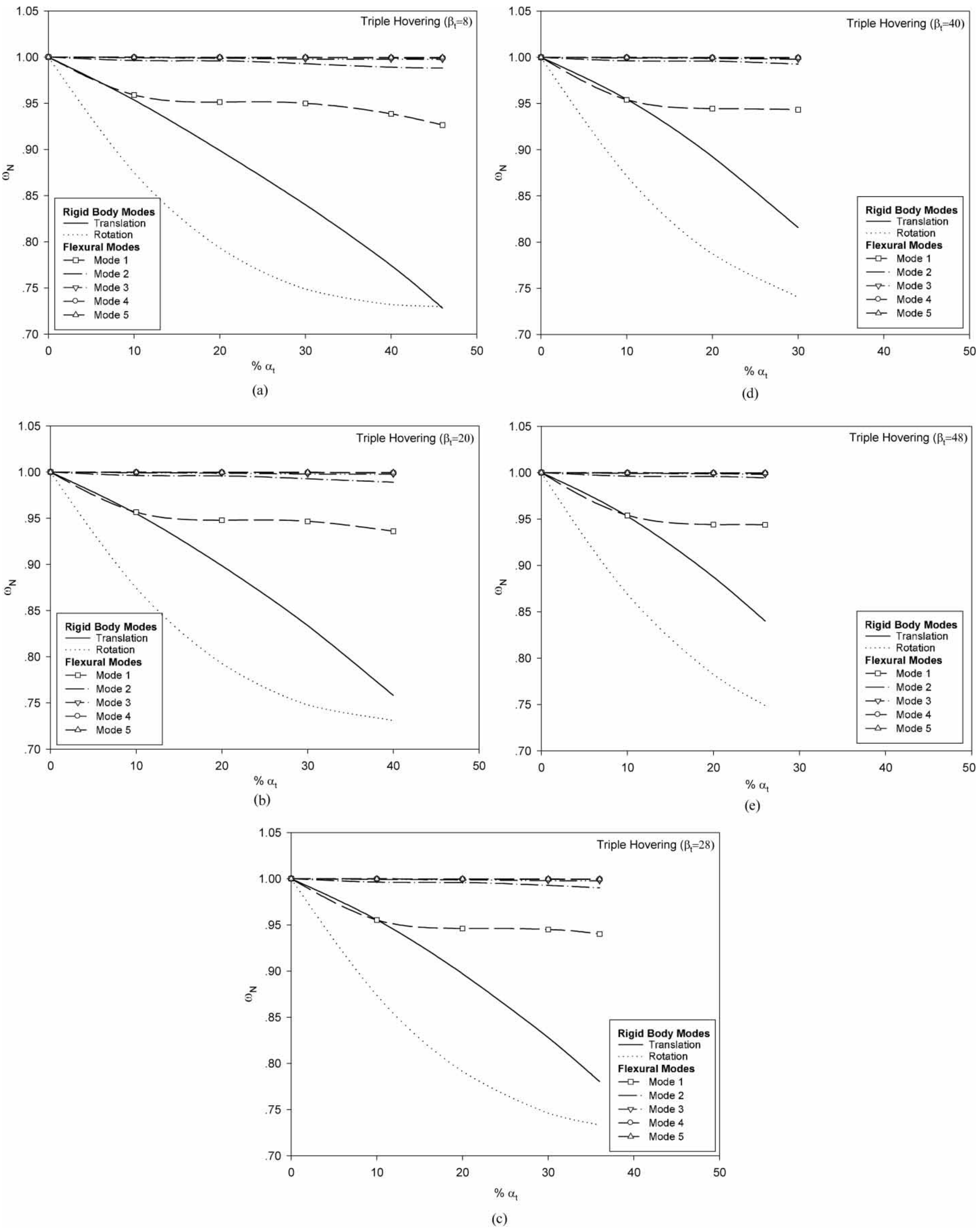

Fig. 9 Effect of triple hanging on natural frequencies of an *in situ* railway concrete sleeper: (a) 8 per cent central void ($\beta_t = 8$ per cent), (b) 20 per cent central void ($\beta_t = 20$ per cent), (c) 28 per cent central void ($\beta_t = 28$ per cent), (d) 40 per cent central void ($\beta_t = 40$ per cent), and (e) 48 per cent central void ($\beta_t = 48$ per cent)

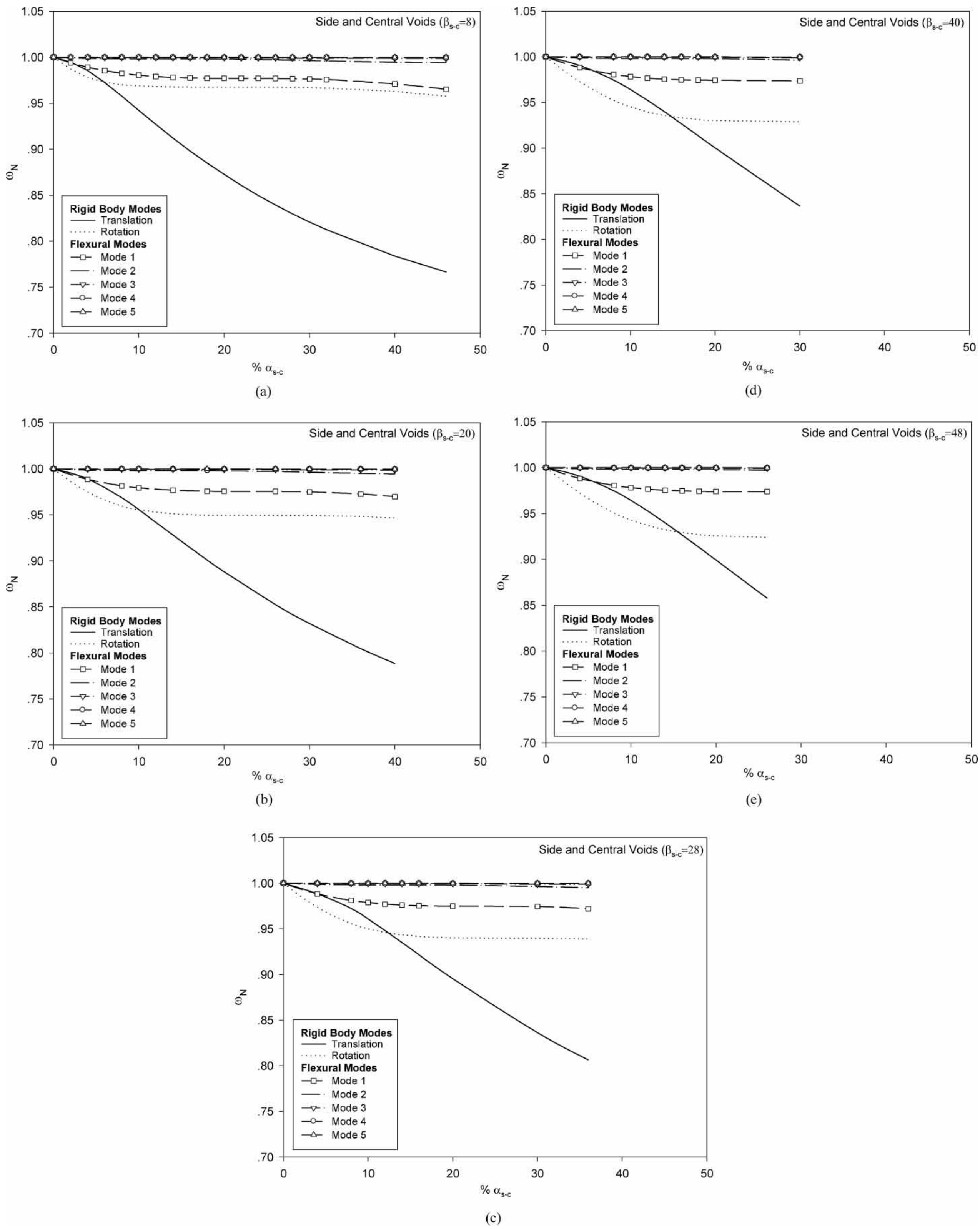

Fig. 10 Effect of side and central voids on natural frequencies of an *in situ* railway concrete sleeper: (a) 8 per cent central void ($\beta_{s-c} = 8$ per cent), (b) 20 per cent central void ($\beta_{s-c} = 20$ per cent), (c) 28 per cent central void ($\beta_{s-c} = 28$ per cent), (d) 40 per cent central void ($\beta_{s-c} = 40$ per cent), and (e) 48 per cent central void ($\beta_{s-c} = 48$ per cent)

of the central void sizes, β_t. In addition, β_t gives rise to the degrees of softening of the bending modes, even though the highest frequency reduction is greater when β_t is lesser. It is found that the highest decreases are varied in the ranges of 15–30 per cent, 25–30 per cent, 5–8 per cent, 1–2 per cent, and 0.02–1 per cent for the translation, rotation, first, second, and other higher modes, respectively. It is worth to note that for the first bending mode at all cases the degrees of softening are likely to be consistent at the moderate to large size of end voids (α_t). In general, it can be concluded that for the symmetrical contact patterns the dynamic behaviour of the *in situ* sleeper tend to be softer due to the imperfections, decreasing with the larger size of voids or the reduction in the support stiffness. Also, the degrees of dynamic softening are found to change continuously within each case.

5.5 Side and central voids

The changes in dynamic behaviour of the *in situ* railway concrete sleepers due to asymmetrical voids are illustrated in Fig. 10. This contact situation can be considered as a case of transition between the two different types of contact patterns such as central void and single hanging. Figure 10(a) presents the effect of end hanging when the central void β_{s-c} is about 8 per cent. The degrees of dynamic softening in the rigid body modes are likely to be similar to another case when β_{s-c} is higher, as can be seen in Figs 10(b) to (e). It is found that the percent variations of α_{s-c} at which the degree of softening of rotational mode is higher than that of translational mode enhance with the increases of β_{s-c}. The ranges of the softening reductions are between 15 per cent and 25 per cent for translational modes and 5–8 per cent for rotational modes.

Apart from the rigid body dynamics, the degrees of softening are higher for most of flexural modes when β_{s-c} shifts upward. The total softening reductions are about 3–5 per cent for the first bending modes, 0.30–0.60 per cent for the second modes, and about 0.01–1 per cent for the remaining modes. The trends in frequency variations are similar to previous cases. It is found that the contact patterns have certain influence on the dynamic characteristics of dynamic flexural modes, but not substantial.

6 CONCLUSIONS

In general, the *in situ* railway concrete sleepers in ballasted tracks are considered to have an ideal contact between the sleeper and the supporting ballast. However, on some occasions that many problems to both sleepers and track systems can be caused by the voids and pockets that form in the sleeper/ballast contact. The current paper presents the results of free vibration analysis of an *in situ* railway concrete sleeper in a track system that take into consideration the sleeper/ballast contact patterns. The effects of the contact configurations on the free vibration responses of the *in situ* railway concrete sleepers are also described. The dynamic modelling of an *in situ* railway concrete sleeper was done using finite-element method. The verification of the model was carried out experimentally and the very good agreement of the results was found [**5**, **6**, **8**]. A series of parametric studies was carried out by varying the parameters of the sleeper/ballast interaction that would be most practical interest in the dynamic health monitoring of the railway track components.

In summary, for the symmetrical contact patterns, the dynamic behaviour of the *in situ* sleeper in the track system tend to be softened by the sleeper/ballast imperfections. The normalized frequencies decrease with the larger size of voids, which means the reduction of the support stiffness. Also, the degrees of dynamic softening change continuously within each case. The voided contacts have a certain influence on the dynamic characteristics of the flexural modes, but not as substantial as on the rigid body vibrations. The asymmetric boundary conditions have drawn much attention due to their influences on the dynamic properties of the *in situ* sleeper, in particular for the rigid body dynamics, e.g. translation and rotation. Dynamic instability can be detected from the parametric studies. The cross-over (swapping) behaviours prevailing in those asymmetrical support conditions due to the deficiency of the ballast support should be noted and integrated into the modern track monitoring system. It is very important to realize that even though the rigid body modes of the track system or of single damaged concrete sleeper in the track system have insignificant influences in the global dynamic track responses, the deteriorated sleeper support plays a vital role in the resonant response, which may result in the accelerated degradation of the railway track components, for instance, cracks in concrete sleepers, or damage of fastening systems, as usually found in the field investigations [**18–22**]. The fact that the voids significantly affect rigid body motions raises a concern for systems where the rigid body motions also play a key role in the dynamic responses of overall track, the vehicle dynamics (e.g. hunting, rolling, etc.) as well as the local track or train instability. Therefore, the measurements of rigid body motions should also be considered as part of track health monitoring in the future.

ACKNOWLEDGEMENTS

The authors gratefully acknowledge the Australian Cooperative Research Centre for Railway Engineering and Technologies (Rail CRC), for the financial support as part of Project #5/23. The figure of the void problem is the courtesy of Mr Ka Ho Li, Railway Engineer of Scott Wilson Ltd, UK. Many thanks go to Professor Jens Nielsen of Charmers University of Technology, Sweden, for kindly sharing related information. Also, the authors wish to thank the reviewers for the constructive comments and suggestions.

REFERENCES

1 **Grassie, S. L.** and **Cox, S. J.** The dynamic response of railway track with unsupported sleepers. *Proc. Instn Mech. Engrs, Part D: J. Automobile Engineering*, 1985, **199**(D2), 123–135.
2 **Clark, R. A., Dean, P. A., Elkins, J. A.,** and **Newton, S. G.** An investigation into the dynamic effects of railway vehicles running on corrugated rails. *J. Mech. Eng. Sci.*, 1982, **24**, 65–76.
3 **Grassie, S. L.** and **Cox, S. J.** The dynamic response of railway track with flexible sleepers to high frequency vertical excitation. *Proc. Instn Mech. Engrs, Part D: J. Automobile Engineering*, 1984, **198**, 117–124.
4 **Knothe, K.** and **Grassie, S. L.** Modelling of railway track and vehicle/track interaction at high frequencies. *Veh. Syst. Dyn.*, 1993, **22**, 209–262.
5 **Dahlberg, T.** and **Nielsen, J.** Dynamic behaviour of free–free and in-situ concrete railway sleepers. In Proceedings of the International Symposium on Precast Concrete Railway Sleepers, Madrid, Spain, 1991, 14 pages.
6 **Grassie, S. L.** Dynamic modelling of concrete railway sleepers. *J. Sound Vibr.*, 1995, **187**, 799–813.
7 **Kaewunruen, S.** and **Remennikov, A. M.** Applications of experimental modal testing for estimating dynamic properties of structural components. In Proceedings of Australian Structural Engineering Conference 2005, New Castle, Australia, 2005 (CD-ROM), 8 pages.
8 **Kaewunruen, S.** and **Remennikov, A. M.** Sensitivity analysis of free vibration characteristics of an in-situ railway concrete sleeper to variations of rail pad parameters. *J. Sound Vibr.*, 2006, **298**, 453–461.
9 **Plenge, M.** and **Lammering, R.** The dynamics of railway track and subgrade with respect to deteriorated sleeper support. In *System dynamics and long-term behaviour of railway vehicles, track and subgrade* (Eds K. Popp and W. Schiehlen), 2003, pp. 295–314 (Springer Verlag, Berlin, Germany).
10 **Kumaran, G., Menon, D.,** and **Nair, K. K.** Dynamic studies of railtrack sleepers in a track structure system. *J. Sound Vibr.*, 2003, **268**, 485–501.
11 **G+D Computing.** Using STRAND7 introduction to the Strand7 finite element analysis system, G+D Computing Pty Ltd, 2002.
12 **Hetenyi, K.** *Beams on elastic foundation: theory with applications in the fields of civil and mechanical engineering*, 1976 (University of Michigan Press, Michigan, USA).
13 **Iyengar, K. T. S. R.** and **Ramu, S. A.** *Design tables for beams on elastic foundations and related structural problems*, 1979 (Applied Science Publishers Ltd, London, UK).
14 **Weaver, W. Jr, Timoshenko, S. P.,** and **Young, D. H.** *Vibration problems in engineering*, 4th edition, 1990 (John Wiley & Sons, New York, USA).
15 **Cai, Z.** *Modelling of rail track dynamics and wheel/rail interaction*. PhD Thesis, Department of Civil Engineering, Queen's University, Ontario, Canada, 1992.
16 **G+D Computing.** STRAND7 theoretical manual, G+D Computing Pty Ltd, 2005.
17 **Remennikov, A. M.** and **Kaewunruen, S.** Experimental investigation on dynamic sleeper/ballast interaction. *Expl Mech.*, 2006, **46**(1), 57–66.
18 **Kaewunruen, S.** and **Remennikov, A. M.** Field trials for dynamic characteristics of railway track and its components using impact excitation technique. *NDT&E Int.*, 2007, **40**(7), 510–519.
19 **Kaewunruen, S.** and **Remennikov, A. M.** Effect of improper ballast tamping/packing on dynamic behaviours of on-track railway concrete sleeper. *Int. J. Struct. Stab. Dyn.*, 2007, **7**, 167–177.
20 **Kaewunruen, S.** and **Remennikov, A. M.** Influence of voids and pockets on vibration characteristics of railway prestressed concrete sleepers. In Proceedings of SEM Annual Conference on Experimental Mechanics, Massachusetts, USA, 2007 (CD-ROM), 10 pages.
21 **Remennikov, A. M.** and **Kaewunruen, S.** A review on loading conditions for railway track structures due to train and track vertical interaction. *Prog. Struct. Eng. Mater.*, 2007, in press.
22 **Barke, D. W.** and **Chiu, W. K.** A review of the effects of out-of-round wheels on track and vehicle components. *Proc. IMechE, Part F: J. Rail and Rapid Transit*, 2005, **219**, 151–175.

APPENDIX

Notation

c_b	damping constant of ballast support system
c_p	damping constant of rail pads
EI	effective sleeper flexural rigidity
EI_c	sleeper flexural rigidity at centre
EI_r	sleeper flexural rigidity at rail seats
k_b	stiffness of ballast support system
k_e	effective stiffness
k_p	rail pad stiffness
k_r	rail stiffness
L	total length of sleeper
L_c	total length of central void
L_s	total length of single hanging void
L_t	length of the left and right-hand side of triple-side hanging voids
L_{dL}	length of the left-hand side of double-side hanging voids
L_{dR}	length of the right-hand side of double-side hanging voids
L_{tC}	length of the central void of triple-side hanging voids
m_s	sleeper mass per unit length

r_s	radius of gyration of sleeper cross-section
$z(x, t)$	vertical deflection of sleeper
$\alpha_c = L_c/L$	ratio of central void length to total sleeper length
$\alpha_s = L_s/L$	ratio of single-side void lengths to total sleeper length
$\alpha_d = L_{dL}/L$	ratio of the left-side void length in double hanging to total sleeper length
$\alpha_t = L_t/L$	ratio of the left/right-side void length in triple hanging to total sleeper length
$\alpha_{s-c} = L_s/L$	ratio of the left-side void length in side-centre voids to total sleeper length
$\beta_d = L_{dR}/L$	ratio of the right-side void length in double hanging to total sleeper length
$\beta_t = L_{tc}/L$	ratio of the central void length in triple hanging to total sleeper length
$\beta_{s-c} = L_c/L$	ratio of the central void length in side-centre voids to total sleeper length
κGA_c	sleeper shear distortion rigidity at centre
κGA_r	sleeper shear distortion rigidity at rail seats
κGA	effective sleeper shear distortion rigidity
ω_N	normalized frequency
ω_{voided}	natural frequency of specific voided sleeper
ω_{ideal}	natural frequency of generic based sleeper
$\psi(x, t)$	rotation angle of sleeper about neutral axis